

# Numerical Exposure Assessment of a WPT Charger

## Report

Quotation #5220037-B to BURY GmbH & Co KG

Document Version 1.1 / 27th Jun, 2022

**Authors:** David Schäfer, Jan Buchholz, Winfried Simon

---



**IMST GmbH**  
Carl-Friedrich-Gauß-Str. 2-4  
47475 Kamp-Lintfort  
Germany




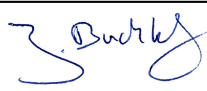

## Information

<b>File Name</b>	Report_15W-WLC-MLBEvo_V1.1.pdf
<b>Initial Date</b>	11th May, 2022
<b>Page count</b>	25

## Versions

Release Date	Version	Author	Comments
11th May, 2022	1.0	David Schäfer	Initial version
27th Jun, 2022	1.1	David Schäfer	Added note about H-field validation

## Approval

Name	Job Title	Date	Signature
David Schäfer	Project leader, simulations	27th Jun, 2022	
Jan Buchholz	Simulations	27th Jun, 2022	
Winfried Simon	Team leader "EM Modeling"	27th Jun, 2022	

## Device Under Test (DUT)

<b>Type of DUT</b>	Wireless Power Transfer Charger
<b>Model Name</b>	15W WLC MLBEvo
<b>FCC ID</b>	QZ9-15WWLC
<b>ISED Certification No.</b>	5927A-15WWLC
<b>Frequency Band</b>	128 kHz
<b>Antennas / Coils / Active Elements</b>	Three coils
<b>Applicant</b>	BURY GmbH & Co KG Robert-Koch-Str. 1-7 32584 Löhne, Germany Contact: Johann Dshus

## Human Exposure Limits

### Specific Absorption Rate (ICNIRP 2020, 1999/519/EC, RPS S-1)

Condition	Uncontrolled Environment (General Public)		Controlled Environment (Occupational)	
	SAR Limit	Mass Avg.	SAR Limit	Mass Avg.
SAR averaged over the whole body mass	0.08 W/kg	whole body	0.4 W/kg	whole body
Peak spatially-averaged SAR for the head, neck & trunk	2.0 W/kg	10 g of tissue*	10 W/kg	10 g of tissue*
Peak spatially-averaged SAR in the limbs/extremities	4.0 W/kg	10 g of tissue*	20 W/kg	10 g of tissue*
*: Defined as a tissue volume in the shape of a cube				

### Specific Absorption Rate (RSS-102 Issue 5)

Condition	Uncontrolled Environment (General Public)		Controlled Environment (Occupational)	
	SAR Limit	Mass Avg.	SAR Limit	Mass Avg.
SAR averaged over the whole body mass	0.08 W/kg	whole body	0.4 W/kg	whole body
Peak spatially-averaged SAR for the head, neck & trunk	1.6 W/kg	1 g of tissue*	8 W/kg	1 g of tissue*
Peak spatially-averaged SAR in the limbs/extremities	4.0 W/kg	10 g of tissue*	20 W/kg	10 g of tissue*
*: Defined as a tissue volume in the shape of a cube				

### Specific Absorption Rate (47 CFR Ch. I § 1.1310 10-1-20 Edition)

Condition	Uncontrolled Environment (General Public)		Controlled Environment (Occupational)	
	SAR Limit	Mass Avg.	SAR Limit	Mass Avg.
SAR averaged over the whole body mass	0.08 W/kg	whole body	0.4 W/kg	whole body
Peak spatially-averaged SAR	1.6 W/kg	1 g of tissue*	8 W/kg	1 g of tissue*
Peak spatially-averaged SAR for extremities, such as hands, wrists, feet, ankles, and pinnae	4.0 W/kg	10 g of tissue*	20 W/kg	10 g of tissue*
*: Defined as a tissue volume in the shape of a cube				

## Internal Electric Field (ICNIRP 2020, RSS-102 Issue 5, RPS S-1)

Condition	Uncontrolled Environment (General Public) EIAV Limit	Controlled Environment (Occupational) EIAV Limit
Peak EIAV @ f (in Hz)	$1.35 \cdot 10^{-4} \cdot f$ V/m	$2.7 \cdot 10^{-4} \cdot f$ V/m
Peak EIAV @ 128 kHz	17.28 V/m	34.56 V/m

## Frequency Scopes

Regulation	SAR		EIAV
	local	whole body	
ICNIRP 2020	100 kHz – 6 GHz	100 kHz – 300 GHz	100 kHz – 10 MHz
47 CFR § 1.1310	100 kHz – 6 GHz		—*
RSS-102 Issue 5	100 kHz – 6 GHz		3 kHz – 10 MHz
1999/ 519/EC	100 kHz – 10 GHz		—
RPS S-1	100 kHz – 6 GHz	100 kHz – 300 GHz	100 kHz – 10 MHz

\*: Not applicable combinations were indicated as "—"

## Evaluation Results

Quantity inside flat phantom	Result*	Below exposure limit set by ...				
		ICNIRP 2020	47 CFR § 1.1310	RSS-102 Issue 5	1999/ 519/EC	RPS S-1
$SAR_{1g, max}$	55.3361 mW/kg	—**	Yes	Yes	—	—
$SAR_{10g, max}$	26.1512 mW/kg	Yes	Yes	Yes	Yes	Yes
$EIAV_{max}$	13.0176 V/m	Yes	—	Yes	—	Yes

\*: Simulated values for "reported model", cf. section 3.2  
 \*\*: Not applicable combinations were indicated as "—"

## Contents

<b>1</b>	<b>Introduction</b>	<b>6</b>
1.1	Objective . . . . .	6
1.2	Simulation Method . . . . .	6
1.3	DUT Description . . . . .	6
1.4	Setup for Reference Measurement . . . . .	6
<b>2</b>	<b>EM Simulation Model</b>	<b>8</b>
2.1	Model Setup . . . . .	8
2.2	Model Check . . . . .	10
2.2.1	Magnetic Fields . . . . .	10
2.2.2	Coil Inductance . . . . .	11
2.2.3	Conclusion of Model Check . . . . .	11
<b>3</b>	<b>SAR and EIAV Evaluation</b>	<b>12</b>
3.1	Simulation Results . . . . .	12
3.2	Simulation Uncertainty . . . . .	14
3.2.1	Simulation Parameter Related Uncertainty . . . . .	14
3.2.2	Model Related Uncertainty . . . . .	17
3.2.3	Model Validation . . . . .	18
3.2.4	Uncertainty Budget . . . . .	19
3.2.5	Uncertainty Penalty . . . . .	20
3.3	Passive Receiver Impact . . . . .	20
3.4	Conclusion of SAR Evaluation . . . . .	22
<b>4</b>	<b>Appendix</b>	<b>23</b>
4.1	Specific Information for Computational Modelling . . . . .	23
4.2	Abbreviations . . . . .	24
<b>5</b>	<b>References</b>	<b>25</b>

## List of Figures

1	Photo of the DUT . . . . .	7
2	Measurement setup CTC . . . . .	7
3	Geometry of the model - outer . . . . .	8
4	Geometry of the model - internal . . . . .	9
5	Geometry of the model - exploded . . . . .	9

6	Magnetic field plane . . . . .	10
7	Line evaluation, graph . . . . .	11
8	Geometry of the phantom . . . . .	12
9	Simulated 1g-averaged SAR results . . . . .	13
10	Simulated EIAV results . . . . .	14
11	Geometry of the passive receiver dummy . . . . .	21
12	EIAV for the model with the passive receiver dummy . . . . .	21

## List of Tables

1	Measured and simulated inductance. . . . .	11
2	SAR and EIAV maximum values . . . . .	12
3	Uncertainty Budget Procedure . . . . .	15
4	SAR and EIAV results for different phantom positions . . . . .	15
5	SAR and EIAV results for different mesh resolutions . . . . .	15
6	SAR and EIAV results for different simulation domain sizes . . . . .	16
7	SAR and EIAV results for different number of total time steps . . . . .	16
8	Uncertainty budget, simulation parameters, 1g-SAR . . . . .	16
9	Uncertainty budget, simulation parameters, 10g-SAR . . . . .	17
10	Uncertainty budget, simulation parameters, EIAV . . . . .	17
11	Uncertainty budget, model setup . . . . .	18
12	Combined and expanded uncertainty, 1g-SAR . . . . .	19
13	Combined and expanded uncertainty, 10g-SAR . . . . .	19
14	Combined and expanded uncertainty, EIAV . . . . .	20
16	Abbreviations . . . . .	24

# 1 Introduction

## 1.1 Objective

The objective is the numerical exposure assessment of one Wireless Power Transfer (WPT) charger (further referred to as "device under test" or "DUT") designed by BURY GmbH & Co KG (further referred to as "applicant"). In particular the Specific Absorption Rate (SAR, thermal hazard) and the internal electric field (EIAV<sup>1</sup>, instantaneous nerve stimulation hazard) were investigated and compared to the exposure limits specified by ICNIRP [1], FCC [2], ISED [3], EUCO [4] and the ARPANSA [5].

## 1.2 Simulation Method

All simulations were done with the Finite Difference Time Domain (FDTD) simulation tool Empire XPU [6]. A numerical model of the DUT was generated and validated by measurements of the magnetic field in its vicinity and measured inductance of the charging coil. The SAR and EIAV inside a flat phantom (human body part model) was investigated similar to the assessment procedures described in IEC/IEEE 62704-1 [7, 8]. The procedures were adapted to make them suitable for the low frequency of the DUT.

## 1.3 DUT Description

The 15 W, triple coil, wireless power charger "15W WLC MLBEvo" (further referred to as "device under test" or "DUT") can be used to charge portable devices like smart-phones (further referred to as "WPT receiver"). It is designed to be integrated into a vehicle, e.g. into the center console of a car. The DUT operates at a frequency of 128 kHz and features three charging coils. During operation only one of the three coils is excited/charging at a time. Which coil is used for charging is chosen by the DUT itself, depending on the placement of the WPT receiver device. A photo of the DUT is depicted in Figure 1.

## 1.4 Setup for Reference Measurement

A validation of the numerical model was carried out by comparing the simulated magnetic field in the vicinity of the DUT with a reference measurement. The measurement was done on the behalf of the applicant by the lab of "CTC advanced GmbH" with the setup depicted in Figure 2. They used a "DASY8" positioner system from Speag and a "MAGPy-H3D" magnetic field probe with a 1 cm<sup>2</sup> "sensor size (loop)" and 6.6 mm "sensor center to tip distance". The measurements were done for a series production equivalent<sup>2</sup> device, running in a testing operating mode at a fixed coil current of 3.5 A RMS. The applicant pre-determined this to be the maximum expectable coil current during

<sup>1</sup>EIAV is the particular name of the post-processing/visualisation feature in Empire XPU. The averaging is optional and was disabled for this investigation.

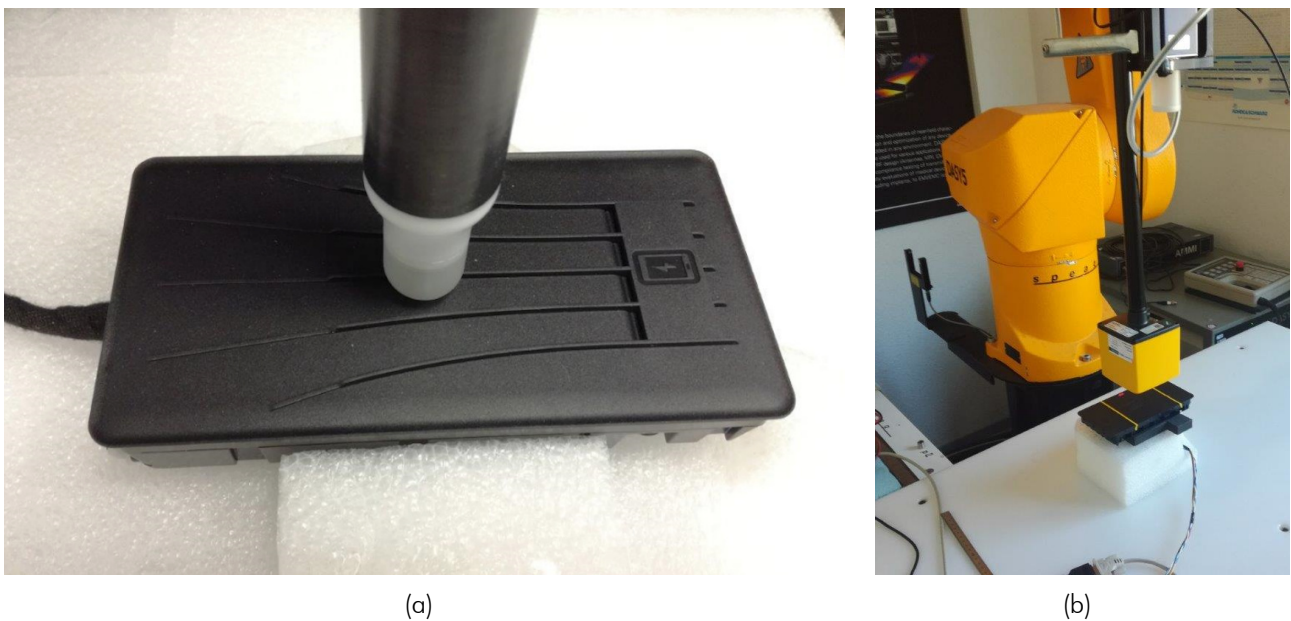
<sup>2</sup>Minor modifications of the dielectric housing and the main PCB routing were done by the applicant after the measurements were executed. We estimate that those modifications are not relevant for the investigated exposure quantities.



**Figure 1:** Photo of the DUT

charging a WPT receiver. No WPT receiver was present during the reference measurements of the magnetic field.

Preliminary measurements showed that the worst-case configuration is given when the center coil is excited, so only this operation state was considered. For the actual reference measurement the field probe was located directly above the  $xy$ -center of the center coil. A line measurement of the magnetic field strength was performed by lifting the probe upwards along the coil axis to different  $z$ -distances from the DUT. Figure 2 (a) show the lowest possible position of the field probe (touch position).



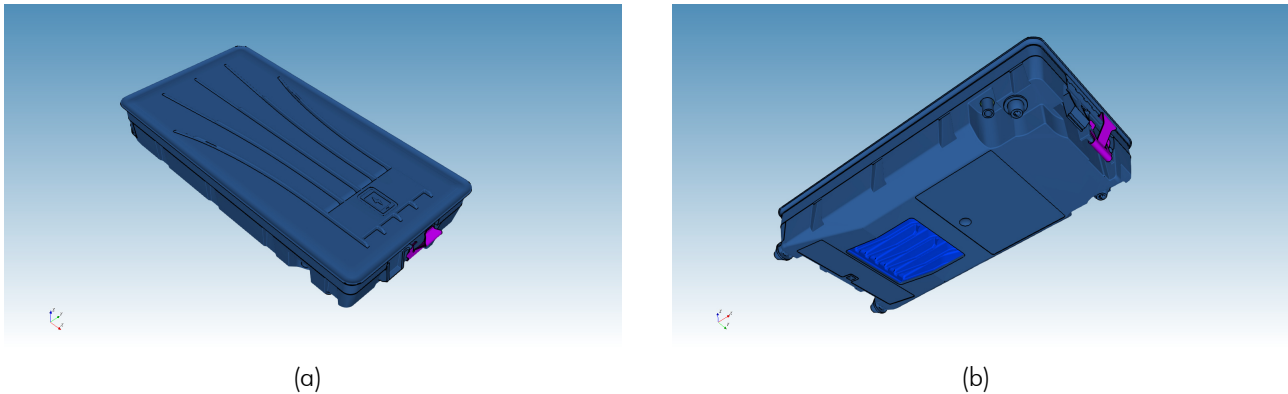
**Figure 2:** Measurement setup from the external lab of "CTC advanced GmbH", showing (a) a close-up of the "MAGPy-H3D" probe in touch position and (b) the "DASY8" positioner (with different probe and DUT).



## 2 EM Simulation Model

### 2.1 Model Setup

The simulation model of the DUT is based on STEP CAD data provided by the applicant. The data was imported into Empire XPU, whereby the coordinate origin of the STEP files was maintained. Figure 3 shows a top and bottom 3D view of the simulation model.



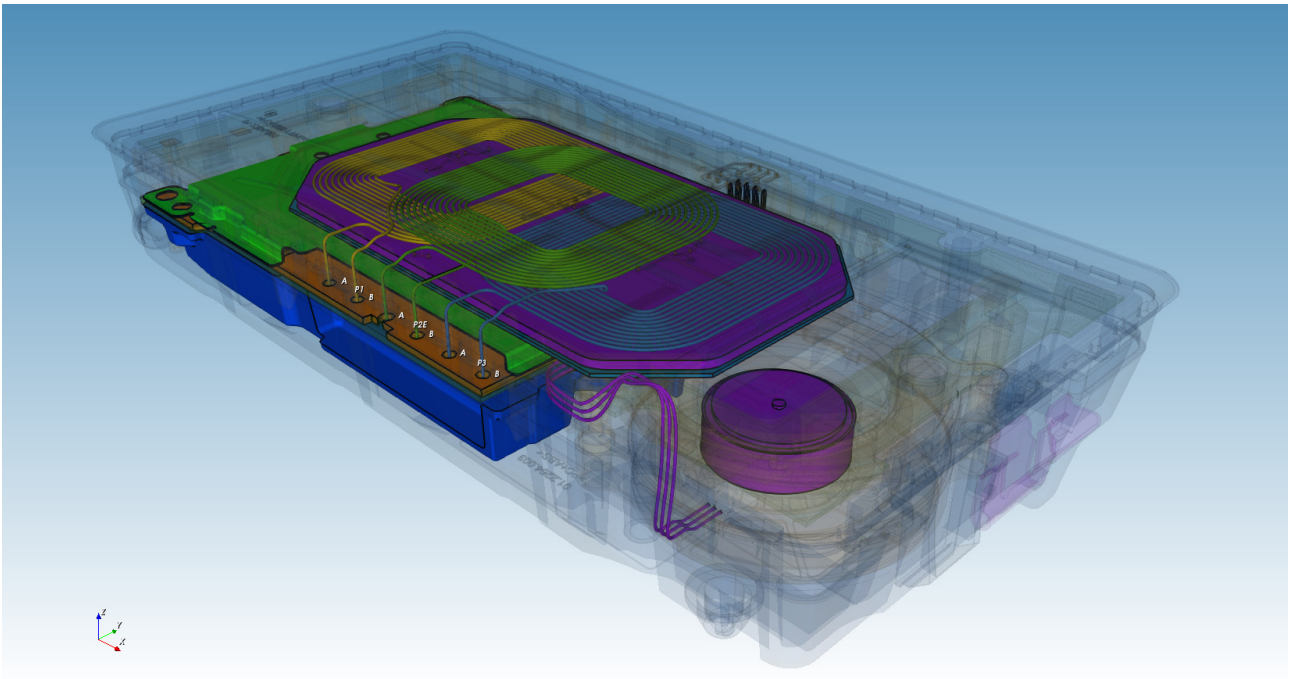
**Figure 3:** Geometry of the Empire simulation model of the DUT, showing the outer view on the top (a) and bottom (b) side.

In Figure 4 the internal components are visible, including the three WPT charging coils. The center coil can be seen in green, located in the middle and overlapping the two sideways coils. Its middle point is located at  $x = y = 0$  mm,  $z = -3.795$  mm and the top side of the DUT housing is at  $z = 2.0$  mm.

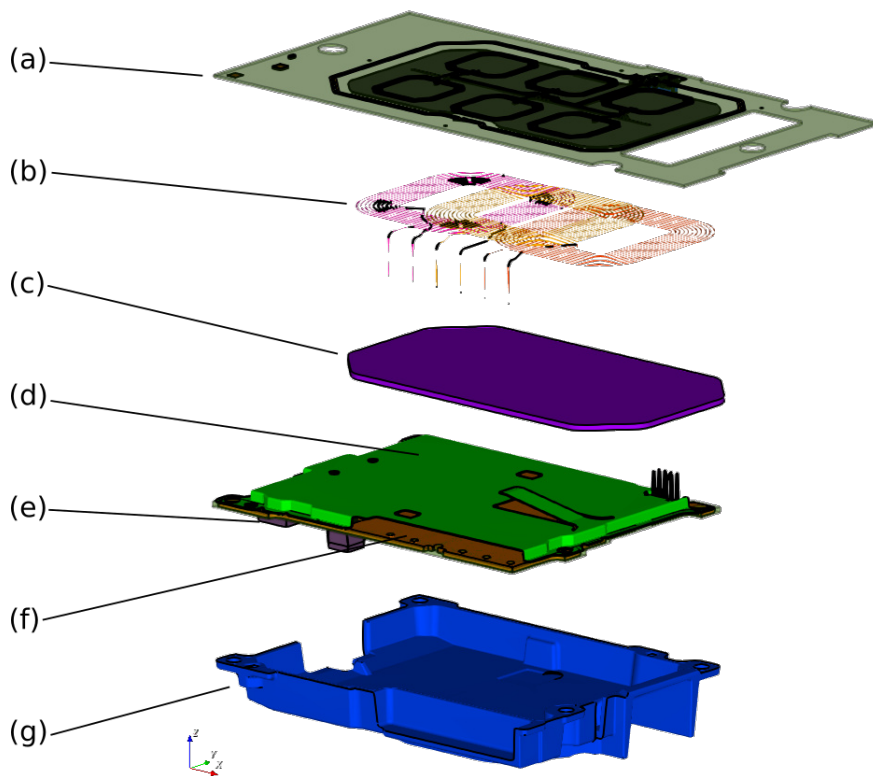
Figure 5 shows an exploded view of the most important components of the simulation model. Based on the applicants information the material properties were set as follows:

- (a) Top PCB (Copper traces,  $\sigma = 57.14857 \cdot 10^6$  S/m)
- (b) WPT coils (Copper,  $\sigma = 56.18 \cdot 10^6$  S/m)
- (c) Ferrite plate ( $\mu_r = 850$ ,  $\tan(\delta) = 0.0153$ )
- (d) Bottom PCB shielding (Steel-Stainless 1.4016 EN),  $\sigma = 1.68 \cdot 10^6$  S/m)
- (e) Bottom PCB components (PEC,  $\sigma = Inf$ )
- (f) Bottom PCB (Copper traces,  $\sigma = 57.14857 \cdot 10^6$  S/m)
- (g) Heat sink (EN AC-47100 = 47100-F,  $AlSi_{12}Cu_1(Fe)$ ,  $\sigma = 17.4 \cdot 10^6$  S/m)

From the top PCB the graphite coating was removed from the simulation model, because it only has a small affect on the assessed quantities.



**Figure 4:** Geometry of the Empire simulation model of the DUT. The housing of the DUT is set transparent to show the internal components.



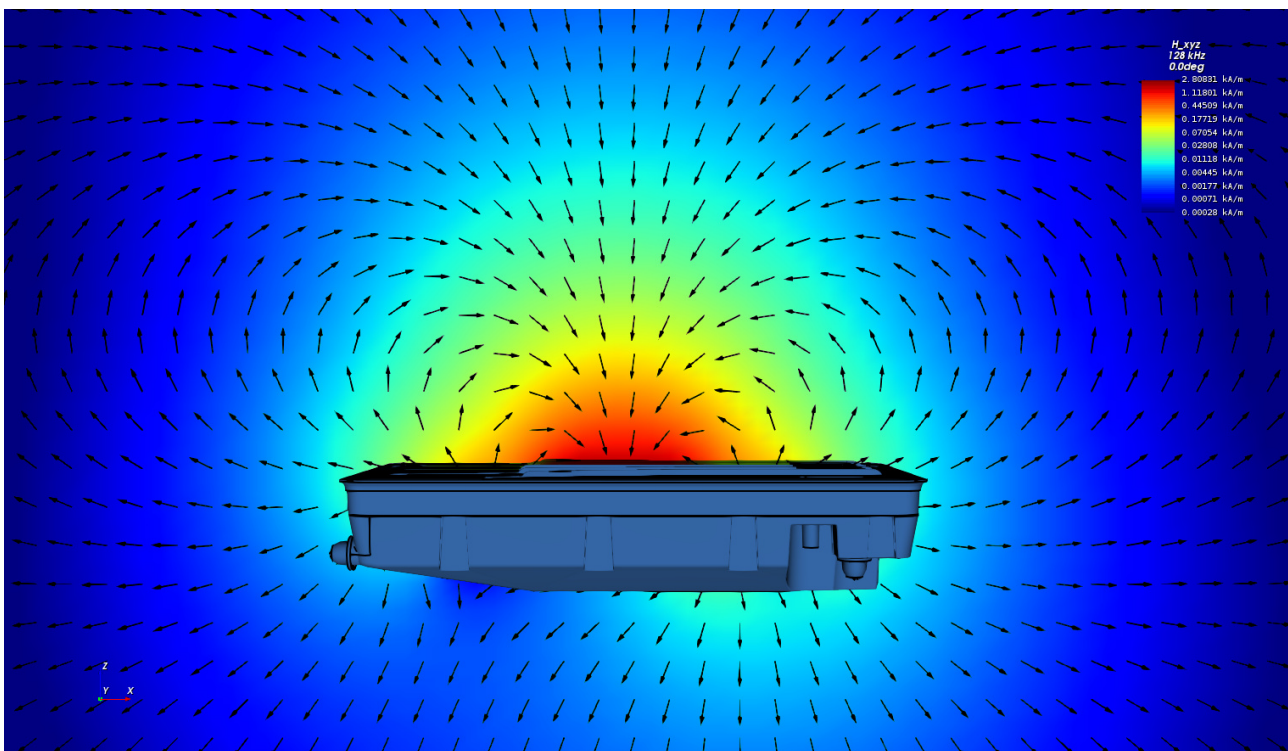
**Figure 5:** Geometry of the Empire simulation model of the DUT, showing an exploded view of the top PCB (a), the WPT coils (b), ferrite (c), bottom PCB shielding (d), bottom PCB components (e), bottom PCB (f) and the heat sink (g).

## 2.2 Model Check

The simulation model was checked by comparing the simulated magnetic fields with the reference measurement (cf. section 1.4). During measurement the central coil was excited with the maximum expectable current of 3.5 A (RMS) at a frequency of 128 kHz. The two sideways coils were inactive, so during the simulation their inputs were terminated with non-excited ports with 1 k $\Omega$  impedance. The simulation setup was unperturbed, meaning that it didn't include a WPT receiver device or phantom (human body model).

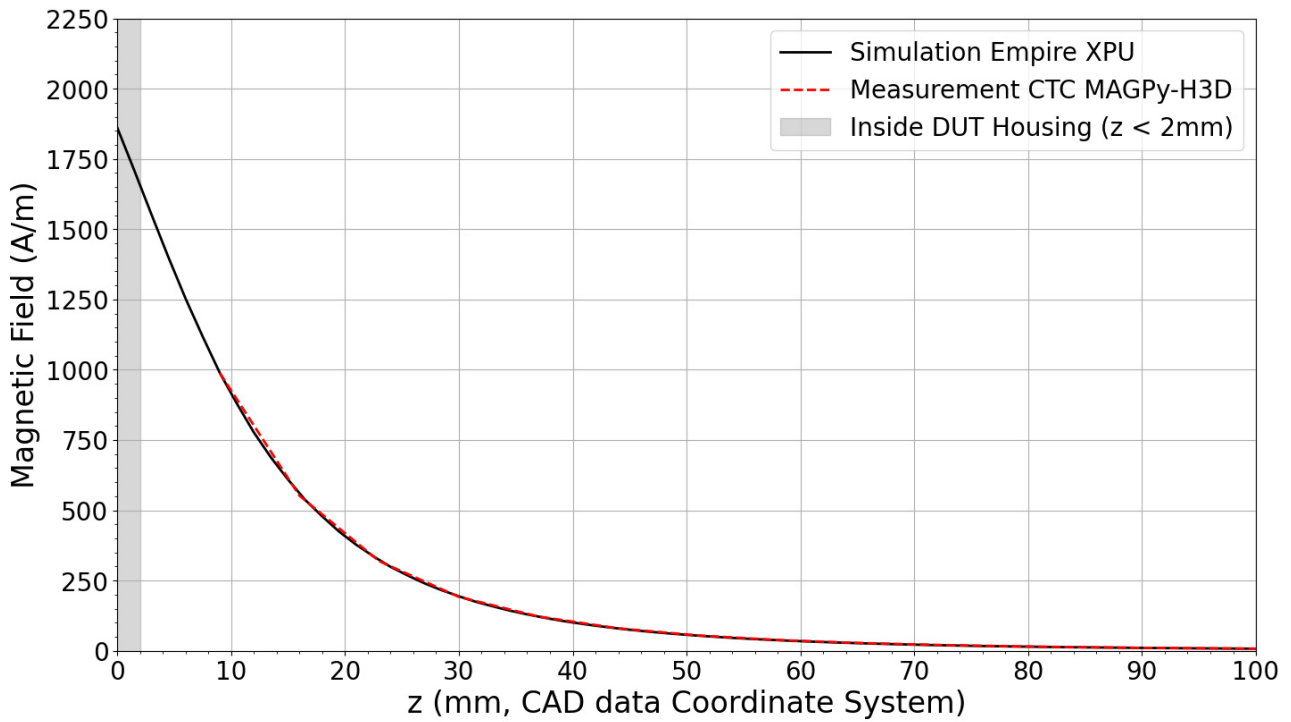
### 2.2.1 Magnetic Fields

Figure 6 shows a  $xz$ -cutplane for the simulated magnetic field strength through the center of the DUT. The colour legend is logarithmic with an 80 dB range. It can be seen how the main PCBs ground and the ferrite confine the main part of the magnetic field to the dedicated WPT receiver location above the DUT.



**Figure 6:** The simulated magnetic field displayed on a  $yz$ -plane through the DUT.

Analogue to the setup of the measurement (cf. section 1.4) the simulated magnetic field (H-field) strength was evaluated along the axis of the central coil. The measurements start at  $z = 2 \text{ mm} + 7 \text{ mm} = 9 \text{ mm}$ , whereby 7 mm approximately corresponds to the "sensor center to tip distance" of the "MAGPy-H3D" field probe. The simulated line starts at  $z = 0 \text{ mm}$  which is 2 mm below the top of the DUTs housing. As Figure 7 depicts, the simulated H-field is in very good agreement with the measurement.



**Figure 7:** Curves for the line evaluation of the H-field (RMS values). The top of the DUT dielectric housing is located at  $z = 2$  mm.

### 2.2.2 Coil Inductance

In addition to the magnetic fields also the inductance of the coil was used to check the simulation model. The measurement was done by the applicant with the coil module taken out of the DUT. With a relative deviation of  $-7,49\%$  (cf. Table 1) the simulated inductance is in good agreement with the measurement.

	Measured	Empire	Deviation
<b>Coil Inductance</b>	11.127 $\mu$ H	11.96 $\mu$ H	+7,49%

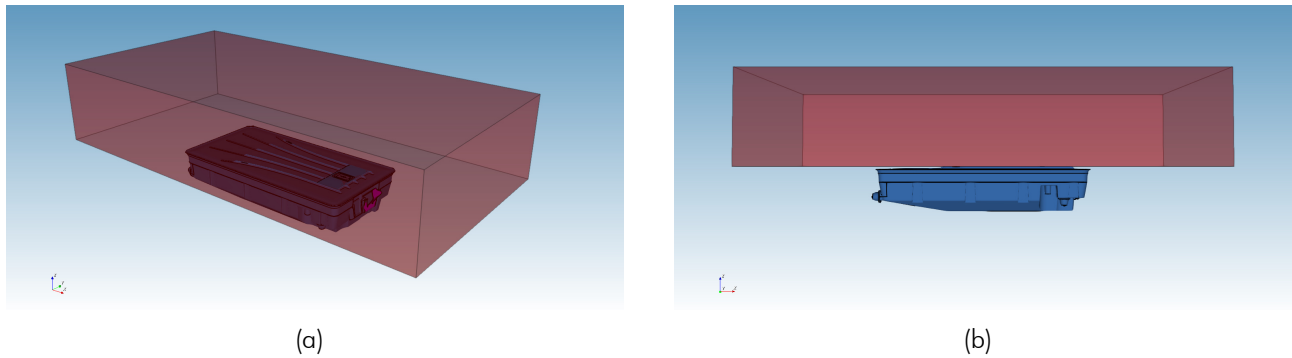
**Table 1:** Measured and simulated inductance.

### 2.2.3 Conclusion of Model Check

It can be concluded, that simulated magnetic field strength and inductance are in good agreement (cf. Figure 7 and Table 1) with the measurements from the applicant and the external lab of "CTC advanced GmbH", indicating the accurate setup of the Empire simulation model.

### 3 SAR and EIAV Evaluation

For the evaluation of the Specific Absorption Rate (SAR) a box shaped flat phantom was added to the simulation model. The setup resembles the situation of someone touching the DUT just after a receiver removal which was in "charging mode" at maximum field. For the SAR evaluation the coil current could have been reduced according to the search mode duty cycle, but with respect to EIAV the continuous maximum expectable coil current was retained throughout the investigation.



**Figure 8:** Geometry of the flat phantom in 3D view (a) and side view (b) showing it is in touch with the DUTs housing.

The phantom was centred ( $xy$ -direction) above the active coil at closest possible  $z$ -distance, virtually touching the top side of the DUT dielectric housing as shown in Figure 8. With respect to the CAD coordinate system origin, the phantom's bottom side (side towards DUT) is located at  $z = 2.0$  mm. The dimensions and the material properties of the phantom are as follows:

1. Geometric Size:  $d_x \cdot d_y \cdot d_z = 360 \text{ mm} \cdot 180 \text{ mm} \cdot 72 \text{ mm}$
2. Relative Permittivity:  $\epsilon_r = 55$
3. Electrical Conductivity:  $\sigma = 0.75 \text{ S/m}$
4. Mass Density:  $\rho = 1000 \text{ kg/m}^3 = 1 \text{ g/cm}^3$

More details about the numerical model, like e.g. domain size, time step or total number of mesh cells, can be found in the appendix in section 4.1.

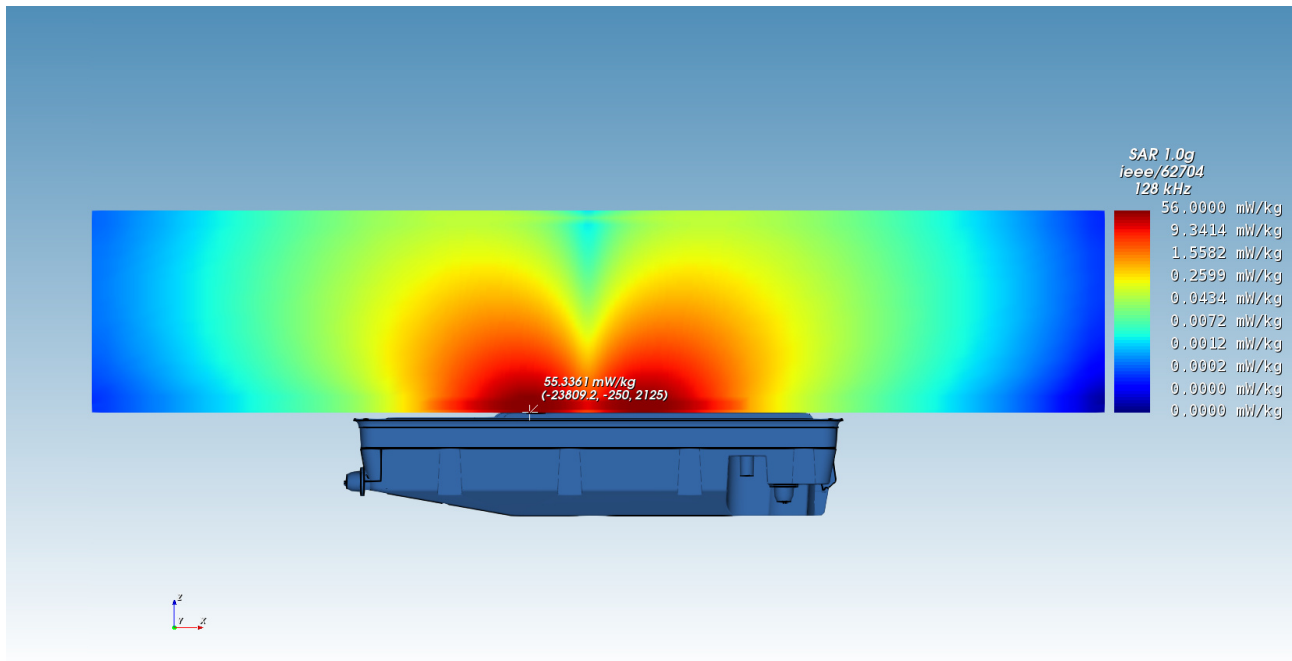
#### 3.1 Simulation Results

Figure 9 shows the simulated 1g- and 10g-averaged SAR and Figure 10 shows the simulated un-averaged EIAV. Table 2 lists the corresponding maximum values and their positions.

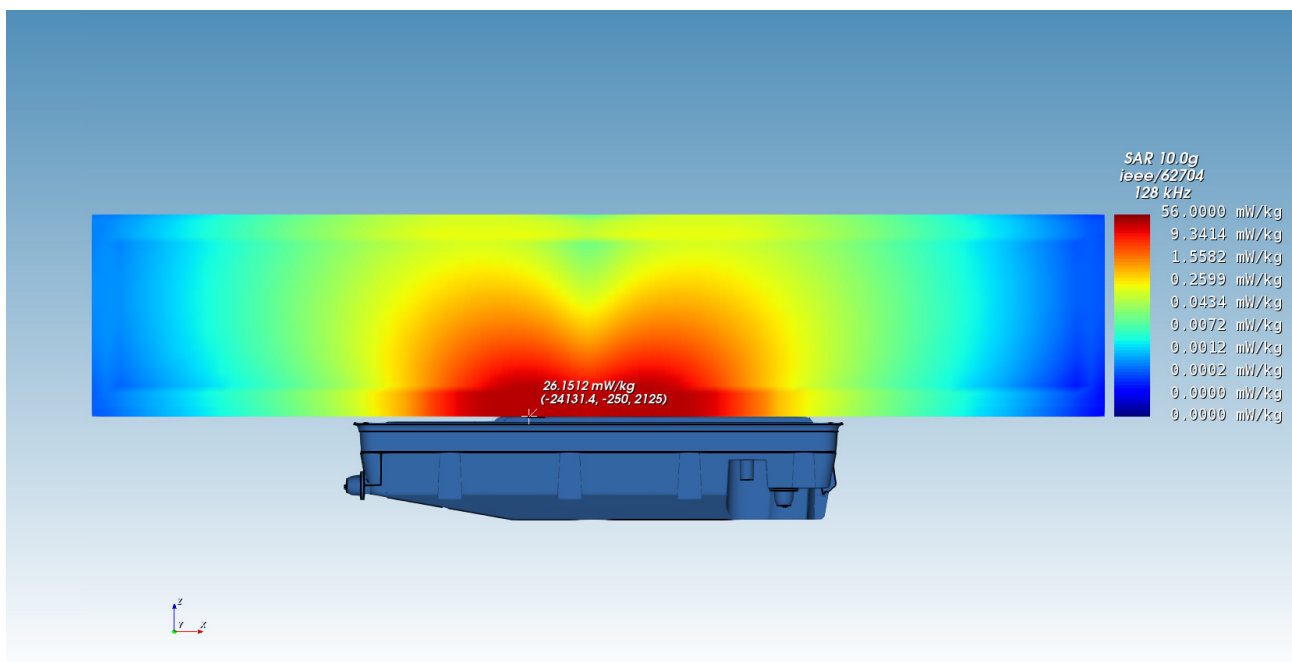
Quantity	Maximum Value	Position of Maximum		
		x	y	z
$\text{SAR}_{1g, \max}$	55.3361 mW/kg	-23.8092 mm	-0.250 mm	2.125 mm
$\text{SAR}_{10g, \max}$	26.1512 mW/kg	-24.1314 mm	-0.250 mm	2.125 mm
$\text{EIAV}_{\text{unaveraged}, \max}$	13.0176 V/m	-23.3576 mm	-0.250 mm	2.125 mm

**Table 2:** SAR and EIAV maximum values with their corresponding positions.



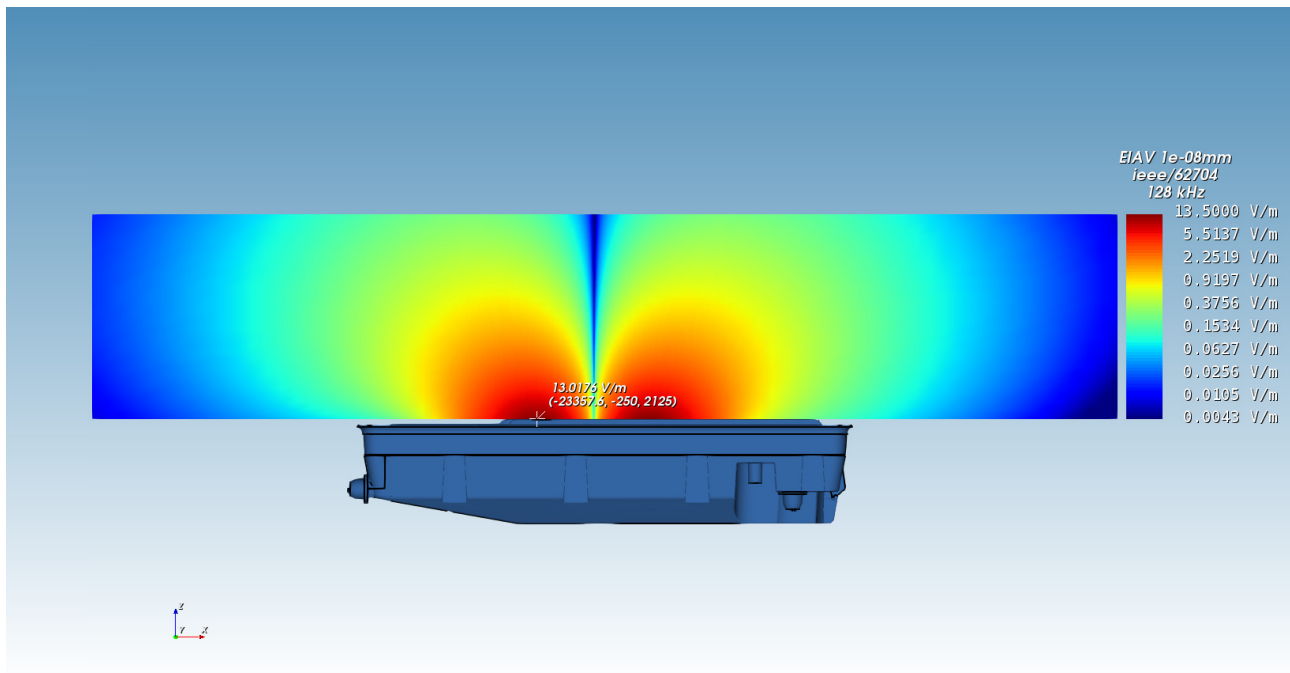


(a) Simulated 1g-averaged SAR



(b) Simulated 10g-averaged SAR

**Figure 9:** Cutplanes through the maxima of the simulated 1g-averaged SAR (a) and 10g-averaged SAR (b) inside the flat phantom. The phantom geometry is not visible. The discontinuities at the phantom boundaries are caused by the averaging algorithm (cf. [7, Section 6.2.2]).



**Figure 10:** Cutplane through the maximum of the simulated EIAV inside the flat phantom. The phantom geometry is not visible.

## 3.2 Simulation Uncertainty

Based on chapter 7 of IEC/IEEE 62704-1 [7] the Combined- and Expanded Standard Uncertainty was calculated to analyse the accuracy of the results for the numerical model (further referred to as "reported model"). Because the DUTs operating frequency is below the scope of the standard, the procedure had to be modified. Details about this will be described in the following sections.

### 3.2.1 Simulation Parameter Related Uncertainty

The procedure for evaluating the simulation parameter related uncertainty (IEC/IEEE 62704-1 [7, section 7.2]) was modified as described in Table 3. Table 4, 5, 6 and 7 show the maximum SAR and EIAV for the investigated variants as well as their relative deviation from the reported model. Table 8, 9 and 10 show the budget of the SAR and EIAV uncertainty contributions of the simulation parameters.

Uncertainty Component	Applicability of the Procedure from IEC/IEEE 62704-1 [7, section 7.2]	Nr. of Variations
Positioning	Applicable. Variation will be: Increase of distance between phantom and DUT by +1 mesh step	1
Mesh Resolution	Not 1:1 applicable. Requested refinement is not practicable at 128 kHz. Instead, total number of mesh cells will be increased by a factor of 2	1
Boundary Condition	Not 1:1 applicable, because $\lambda/4$ (=585.5 m) is way too large at 128 kHz. Instead, simulation domain will be enlarged by 50% simultaneously in +/- x/y/z direction	1
Power Budget	Not applicable. No travelling wave conditions are given, so comparison with power absorbed in ABC is not possible. Excitation will be normalized to fixed port/coil current.	0
Convergence	Not 1:1 applicable. Instead, variation will be simulated longer by a factor of 1.5 or more.	1
Phantom dielectrics	Not applicable / not indicated because fixed permittivity and conductivity from IEC/TR 62905 were used.	0

**Table 3:** Description of the modified procedure for obtaining the uncertainty budget.

Phantom z-Position	2 mm	2.25 mm
SAR <sub>1g, max</sub>	55.3361 mW/kg	52.9025 mW/kg
SAR <sub>10g, max</sub>	26.1512 mW/kg	25.1301 mW/kg
EIAV <sub>max</sub>	13.0176 V/m	12.7051 V/m
SAR <sub>1g, max</sub> -Deviation	0 %	-4.40 %
SAR <sub>10g, max</sub> -Deviation	0 %	-3.90 %
EIAV-Deviation	0 %	-2.40 %

**Table 4:** SAR and EIAV results for different phantom positions. The first data column corresponds to the reported model (cf. section 3.1).

Mesh Resolution	5.7 MCells	12.1 MCells
SAR <sub>1g, max</sub>	55.3361 mW/kg	56.0547 mW/kg
SAR <sub>10g, max</sub>	26.1512 mW/kg	26.4064 mW/kg
EIAV <sub>max</sub>	13.0176 V/m	13.1848 V/m
SAR <sub>1g, max</sub> -Deviation	0 %	1.30 %
SAR <sub>10g, max</sub> -Deviation	0 %	0.98 %
EIAV-Deviation	0 %	1.28 %

**Table 5:** SAR and EIAV results for different mesh resolutions. The first data column corresponds to the reported model (cf. section 3.1).



Domain Size	560 · 380 · 408 mm	1120 · 760 · 816 mm
SAR <sub>1g, max</sub>	55.3361 mW/kg	55.3253 mW/kg
SAR <sub>10g, max</sub>	26.1512 mW/kg	26.1434 mW/kg
EIAV <sub>max</sub>	13.0176 V/m	13.0154 V/m
SAR <sub>1g, max</sub> -Deviation	0 %	-0.02 %
SAR <sub>10g, max</sub> -Deviation	0 %	-0.03 %
EIAV-Deviation	0 %	-0.02 %

**Table 6:** SAR and EIAV results for different simulation domain sizes. The first data column corresponds to the reported model (cf. section 3.1). The simulation domain was enlarged symmetrically in all spatial directions.

Time/Convergence	20 Msteps	40 Msteps
Energy Decay	-103.98 dB	-104.46 dB
SAR <sub>1g, max</sub>	55.3361 mW/kg	55.3338 mW/kg
SAR <sub>10g, max</sub>	26.1512 mW/kg	26.1497 mW/kg
EIAV <sub>max</sub>	13.0176 V/m	13.0158 V/m
SAR <sub>1g, max</sub> -Deviation	0 %	-0.00 %
SAR <sub>10g, max</sub> -Deviation	0 %	-0.01 %
EIAV-Deviation	0 %	-0.01 %

**Table 7:** SAR and EIAV results for different number of total time steps. The first data column corresponds to the reported model (cf. section 3.1).

Uncertainty Component	Section in [7]	1g-SAR Tolerance in %	Probability Distribution	Divisor	$c_i$	1g-SAR Uncertainty in %
Positioning	7.2.1	-4.40 %	R	1.73	1	-2.54 %
Mesh Resolution	7.2.2	1.30 %	N	1	1	1.30 %
Boundary Condition	7.2.3	-0.02 %	N	1	1	-0.02 %
Power Budget	7.2.4	<i>not appl.</i>	N	1	1	<i>not appl.</i>
Convergence	7.2.5	-0.00 %	R	1.73	1	-0.00 %
Phantom dielectrics	7.2.6	<i>not appl.</i>	R	1.73	1	<i>not appl.</i>
<b>Combined Std. Uncertainty (k=1)</b>						<b>2.85 %</b>

**Table 8:** Budget of the 1g-SAR uncertainty contributions of the simulation parameters, corresponding to IEC/IEEE 62704-1 [7, Table 3]. Note: N, R, U = normal, rectangular, U-shaped probability distributions.

Uncertainty Component	Section in [7]	10g-SAR Tolerance in %	Probability Distribution	Divisor	$c_i$	10g-SAR Uncertainty in %
Positioning	7.2.1	-3.90 %	R	1.73	1	-2.26 %
Mesh Resolution	7.2.2	0.98 %	N	1	1	0.98 %
Boundary Condition	7.2.3	-0.03 %	N	1	1	-0.03 %
Power Budget	7.2.4	<i>not appl.</i>	N	1	1	<i>not appl.</i>
Convergence	7.2.5	-0.01 %	R	1.73	1	-0.00 %
Phantom dielectrics	7.2.6	<i>not appl.</i>	R	1.73	1	<i>not appl.</i>
<b>Combined Std. Uncertainty (k=1)</b>						2.46 %

**Table 9:** Budget of the 10g-SAR uncertainty contributions of the simulation parameters, corresponding to IEC/IEEE 62704-1 [7, Table 3]. Note: N, R, U = normal, rectangular, U-shaped probability distributions.

Uncertainty Component	Section in [7]	EIAV Tolerance in %	Probability Distribution	Divisor	$c_i$	EIAV Uncertainty in %
Positioning	7.2.1	-2.40 %	R	1.73	1	-1.39 %
Mesh Resolution	7.2.2	1.28 %	N	1	1	1.28 %
Boundary Condition	7.2.3	-0.02 %	N	1	1	-0.02 %
Power Budget	7.2.4	<i>not appl.</i>	N	1	1	<i>not appl.</i>
Convergence	7.2.5	-0.01 %	R	1.73	1	-0.01 %
Phantom dielectrics	7.2.6	<i>not appl.</i>	R	1.73	1	<i>not appl.</i>
<b>Combined Std. Uncertainty (k=1)</b>						1.89 %

**Table 10:** Budget of the EIAV uncertainty contributions of the simulation parameters, analogue to the budget of the SAR uncertainty contributions of the simulation parameters to IEC/IEEE 62704-1 [7, Table 3]. Note: N, R, U = normal, rectangular, U-shaped probability distributions.

### 3.2.2 Model Related Uncertainty

For distances  $d < \lambda/2$  the IEC/IEEE 62704-1 [7, section 7.3.3] states that "[...] the only way to determine the uncertainty of the DUT model is by SAR measurements", which is not possible for the given frequency of the DUT. Therefore the procedure was modified by using the squared H-field values instead of SAR in [7, equation 14], similar to the assessment for distances  $d \geq \lambda/2$  by [7, equation 13].

$$U_{\text{sim,model}} = \max \left( \frac{|H_{\text{ref,n}}^2 - H_{\text{sim,n}}^2|}{H_{\text{ref,max}}^2} \right) \quad (1)$$

$$= 1.04 \% \quad (2)$$

In this context, ISED asked for demonstration that the primary E-field does not contribute to the exposure ratio and can therefore be ignored for the evaluation the uncertainty budget. IMST provided corresponding evidence separately by the example of a simplified generic WPT inductive charger. ISED considered the justification provided to be sufficient in the context of this particular application and is currently finalizing its review to determine if the justification can be applied more broadly.

Table 11 shows the budget of the uncertainty contributions of the model parameter. The applicant stated an  $k=2$  uncertainty of 1.24 dB  $\Rightarrow$  15.28 % for the measurements done by CTC advanced (cf. section 1.4), so 7.64 % was used for the  $k=1$  uncertainty of the measurement equipment and procedure.

Uncertainty Component (SAR)	Section in [7]	Tolerance in %	Probability Distribution	Divisor	$c_i$	Uncertainty in %
Uncertainty of the DUT model	7.3.2 or 7.3.3	1.04 %	N	1	1	1.04 %
Uncertainty of the phantom model	7.3.3	<i>not appl.</i>	N	1	1	<i>not appl.</i>
Uncertainty of the measurement equipment and procedure	-	7.64 %	N	1	1	7.64 %
<b>Combined Std. Uncertainty (k=1)</b>						<b>7.71 %</b>

**Table 11:** Budget of the uncertainty contributions of the model setup, corresponding to IEC/IEEE 62704-1 [7, Table 4]. Note: N, R, U = normal, rectangular, U-shaped probability distributions.

### 3.2.3 Model Validation

To validate the numerical model the equation 15 from IEC/IEEE 62704-1 [7, section 7.3.4] was calculated for the H-field line evaluation.

$$E_n = \max \left( \sqrt{\frac{(\nu_{\text{sim,n}} - \nu_{\text{ref,n}})^2}{(\nu_{\text{sim,n}} U_{\text{sim}(k=2)})^2 + (\nu_{\text{ref,n}} U_{\text{ref}(k=2)})^2}} \right) \quad (3)$$

$$= \max \left( \sqrt{\frac{(H_{\text{sim,n}}^2 - H_{\text{ref,n}}^2)^2}{(H_{\text{sim,n}}^2 U_{\text{sim}(k=2)})^2 + (H_{\text{ref,n}}^2 U_{\text{ref}(k=2)})^2}} \right) \quad (4)$$

$$= 0.22 \leq 1 \quad (5)$$

The condition/inequation is fulfilled, indicating that the deviation is within the expected uncertainty, and hence that the model is valid.

### 3.2.4 Uncertainty Budget

The budgets for simulation parameters related uncertainties and model related uncertainties were combined ( $k=1$ ) and expanded ( $k=2$ ) for 1g-SAR, 10g-SAR and EIAV as shown in table 12, 13 and 14.

Uncertainty Component (1g-SAR)	Section in [7]	Tolerance in %	Probability Distribution	Divisor	$c_i$	Uncertainty in %
Uncertainty of the DUT model with respect to simulation parameters	7.2	2.85 %	N	1	1	2.85 %
Uncertainty of the developed numerical model of the DUT	7.3	7.71 %	N	1	1	7.71 %
<b>Combined Std. Uncertainty (<math>k=1</math>)</b>						8.22 %
<b>Expanded Std. Uncertainty (<math>k=2</math>)</b>						16.44 %

**Table 12:** Combined and expanded budget of the 1g-SAR uncertainty, corresponding to IEC/IEEE 62704-1 [7, Table 5]. Note: N, R, U = normal, rectangular, U-shaped probability distributions.

Uncertainty Component (10g-SAR)	Section in [7]	Tolerance in %	Probability Distribution	Divisor	$c_i$	Uncertainty in %
Uncertainty of the DUT model with respect to simulation parameters	7.2	2.46 %	N	1	1	2.46 %
Uncertainty of the developed numerical model of the DUT	7.3	7.71 %	N	1	1	7.71 %
<b>Combined Std. Uncertainty (<math>k=1</math>)</b>						8.09 %
<b>Expanded Std. Uncertainty (<math>k=2</math>)</b>						16.19 %

**Table 13:** Combined and expanded budget of the 10g-SAR uncertainty, corresponding to IEC/IEEE 62704-1 [7, Table 5]. Note: N, R, U = normal, rectangular, U-shaped probability distributions.

Uncertainty Component (EIAV)	Section in [7]	Tolerance in %	Probability Distribution	Divisor	$c_i$	Uncertainty in %
Uncertainty of the DUT model with respect to simulation parameters	7.2	1.89 %	N	1	1	1.89 %
Uncertainty of the developed numerical model of the DUT	7.3	7.71 %	N	1	1	7.71 %
<b>Combined Std. Uncertainty (k=1)</b>						7.94 %
<b>Expanded Std. Uncertainty (k=2)</b>						15.88 %

**Table 14:** Combined and expanded budget of the EIAV uncertainty, analogue to the budget of the SAR uncertainty from IEC/IEEE 62704-1 [7, Table 5]. Note: N, R, U = normal, rectangular, U-shaped probability distributions.

### 3.2.5 Uncertainty Penalty

The calculated Expanded Std. Uncertainties for SAR/EIAV do not exceed the maximum of 30 % stated in IEC/IEEE 62704-1 [7, Section 7.4]. Therefore uncertainty penalties as described in EN 62311 [9, Section 6.2, Equation 1] were not applied.

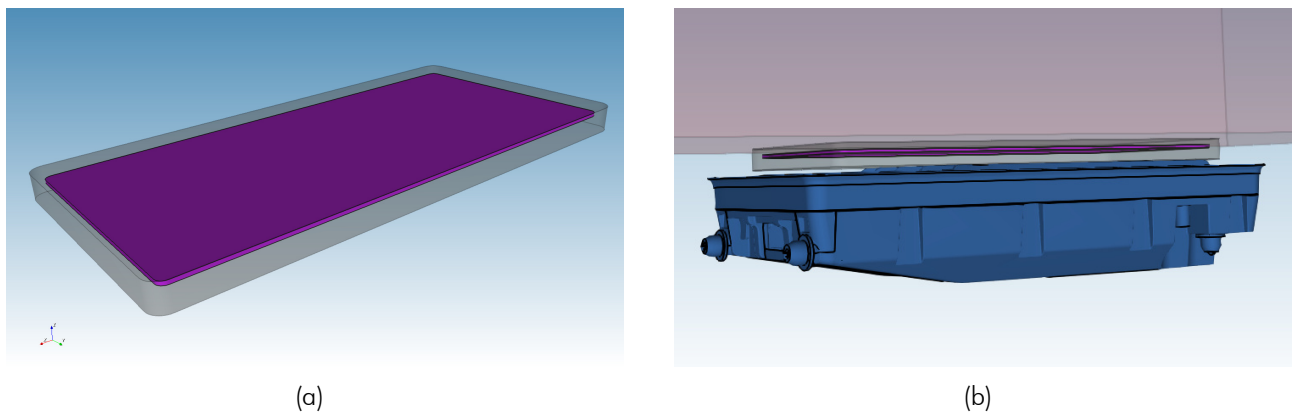
## 3.3 Passive Receiver Impact

In the reported model the phantom is directly placed onto the DUT. However, usually a WPT receiver such as a handset is placed on top of the DUT during charging operation. A receiver would increase the smallest possible approach distance, and its metal parts would act as a shield for the E- and H-fields, hence decreasing the exposure. To illustrate this effect, an additional simulation was done, whereby a passive phone receiver dummy was added to the model (cf. Figure 11).

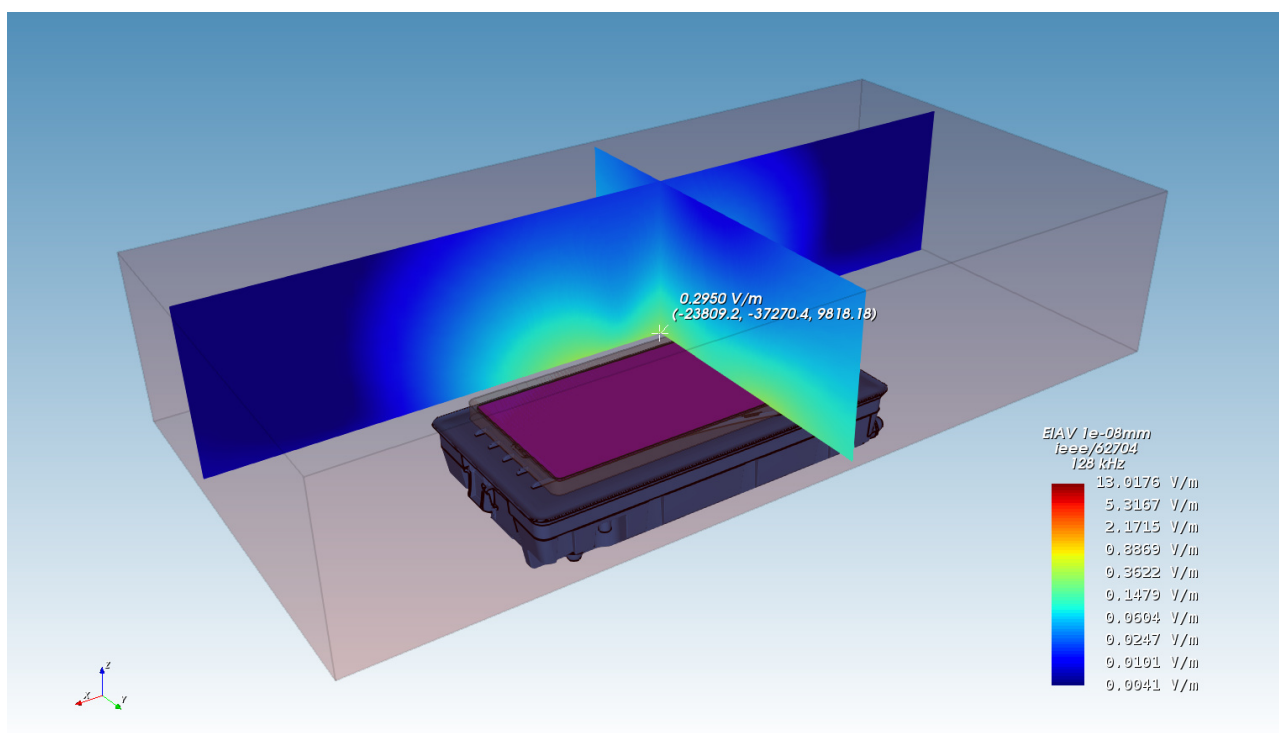
Table 2 lists the maximum values for 1g-SAR, 10g-SAR and EIAV and their positions for model with the passive receiver dummy. As expected they are noticeable lower than in case of the reported model. The before mentioned shielding effect also qualitatively changes the SAR/EIAV distribution, as can be seen in Figure 12.

Quantity	Reported Model	With Passive Receiver
$SAR_{1g, max}$	55.3361 mW/kg	0.036 mW/kg
$SAR_{10g, max}$	26.1512 mW/kg	0.019 mW/kg
$EIAV_{unaveraged, max}$	13.0176 V/m	0.295 V/m

**Table 15:** SAR and EIAV maximum values for the model with the passive receiver dummy.



**Figure 11:** Geometry of the passive receiver dummy, consisting of a 145 · 70 · 7 mm dielectric housing with a metal plate inside (a). The receiver dummy was placed in between DUT and phantom (b).



**Figure 12:** Cutplane through the maximum of the simulated EIAV inside the flat phantom for the model with the passive receiver dummy.

### 3.4 Conclusion of SAR Evaluation

Summarizing the numerical exposure assessment of the DUT, the following can be stated:

1. The simulated magnetic field strength and the coil inductance are in good agreement with the measurements (cf. section 2.2), indicating the accurate setup of the DUT simulation model (without phantom).
2. The investigated scenario (reported model) follows the worst-case assumption that:
  - (a) The flat phantom is in direct contact with the DUT with no receiver in between.
  - (b) The DUT is exciting its center coil with the maximum expectable current, despite the fact that no receiver device is present.
  - (c) The search mode duty cycle is neglected.
3. The model validation (cf. section 3.2.3) shows that in-equation 15 from IEC/IEEE 62704-1 is fulfilled, indicating a valid numerical model.
4. The uncertainty analysis returns Expanded Standard Uncertainties below the permissible 30% stated in IEC/IEEE 62704-1 section 7.4.
5. The evaluated maximum 1g-averaged SAR is 55.3361 mW/kg.
6. The evaluated maximum 10g-averaged SAR is 26.1512 mW/kg.
7. The evaluated maximum EIAV (internal Electric field) is 13.0176 V/m.
8. With respect to the statements above, the conclusion of this numerical exposure assessment report is, that the DUT does not exceed the SAR and/or EIAV exposure limits specified by ICNIRP [1], FCC [2], ISED [3], EUCO [4] and ARPANSA [5]. A tabular evaluation can be found at the beginning of the report.

## 4 Appendix

### 4.1 Specific Information for Computational Modelling

**Computational resources** Computation was performed on an Intel Xeon Platinum 8168 24-core processor with 4.294 GB memory usage.

**FDTD algorithm implementation and validation** cf. [8]

**Computing peak SAR from field components** cf. [8]

**1g-averaged SAR procedures** cf. [7, 8]

**Computational parameters for reported model:**

**Cell Size (min/max):** 0.2216 mm / 10.37 mm

**Domain Size:** 560 · 380 · 408 mm

**Total amount of mesh cells:** approx. 5.7 million

**Time step:**  $2.61002 \cdot 10^{-13}$  s

**Total number of time steps:** approx. 20 million

**Simulation time:** approx. 3 hours and 28 minutes

**Simulation speed:** 9223.324 million cells per second (9.223 GCells/s).

**Excitation method:** Gaussian pulse with  $f_0 = 0$  Hz,  $f_{BW} = 50$  MHz

**Phantom model implementation** cf. section 3

**Tissue dielectric parameters** cf. section 3

**Transmitter model implementation and validation** cf. section 2

**Test device positioning** cf. section 3

**Steady state termination procedures** A Gaussian pulse was used for the excitation and the simulation was terminated when the energy has dissipated to more than 103.98 dB.

**Test results** cf. section 3



## 4.2 Abbreviations

Abbreviation	Description
CAD	Computer Aided Design
DUT	Device Under Test
EIAV	Averaged Internal Electric Field
EM	Electro Magnetic
FDTD	Finite Difference Time Domain
PCB	Printed Circuit Board
RF	Radio Frequency
RMS	Root Mean Square
SAR	Specific Absorption Rate
S/m	Siemens per meter = $1/(\Omega\text{m})$

**Table 16:** Abbreviations.

## 5 References

- [1] International Commission on Non-Ionizing Radiation Protection (ICNIRP), "ICNIRP Guidelines for limiting Exposure to Electromagnetic Fields (100 KHz to 300 GHz)," 2020.
- [2] Federal Communications Commission (FCC, USA), "FCC Limits for Specific Absorption Rate (SAR), 47 C.F.R. § 2.1093," 2012.
- [3] Innovation, Science and Economic Development Canada (ISED, Canada), "RSS-102 Issue 5 - Radio Frequency (RF) Exposure Compliance of Radiocommunication Apparatus (All Frequency Bands)," March 2015.
- [4] European Council, "Council Recommendation of 12 July 1999 on the limitation of exposure of the general public to electromagnetic fields (0 Hz to 300 GHz), 1999/519/EC," July 1999.
- [5] Australian Radiation Protection and Nuclear Safety Agency (ARPANSA), "Standard for Limiting Exposure to Radiofrequency Fields – 100 kHz to 300 GHz - Radiation Protection Series S-1, RPS S-1," February 2021.
- [6] IMST GmbH. (2020, August) Empire XPU. Carl-Friedrich-Gauß-Str. 2-4, 47475 Kamp-Lintfort, Germany. [Online]. Available: <http://empire.de>
- [7] "IEC/IEEE International Standard – Determining the peak spatial-average specific absorption rate (SAR) in the human body from wireless communications devices, 30 MHz to 6 GHz - Part 1: General requirements for using the finite-difference time-domain (FDTD) method for SAR calculations," *IEC/IEEE 62704-1:2017*, pp. 1–86, 2017.
- [8] IMST GmbH, "EMPIRE XPU - Code Verification according to IEC/IEEE P62704-1."
- [9] CENELEC, "Assessment of electronic and electrical equipment related to human exposure restrictions for electromagnetic fields (0 Hz to 300 GHz), EN IEC 62311," January 2020.